Diurnal to Decadal Changes in the Balance between Vegetation and Bare Ground in Tasmanian Fjaeldmark

Authors: Annandale, Bryan, and Kirkpatrick, Jamie B.

Source: Arctic, Antarctic, and Alpine Research, 49(3) : 473-486

Published By: Institute of Arctic and Alpine Research (INSTAAR), University of Colorado

URL: https://doi.org/10.1657/AAAR0017-001

Arctic, Antarctic, and Alpine Research, Vol. 49, No. 3, 2017, pp. 473–486
DOI: http://dx.doi.org/10.1657/AAAR0017-001

Diurnal to decadal changes in the balance between vegetation and bare ground in Tasmanian fjaeldmark

Bryan Annandale[1,*] and Jamie B. Kirkpatrick[1]

[1]Discipline of Geography and Spatial Sciences, School of Land and Food, University of Tasmania, Private Bag 78, GPO, Hobart, Tasmania 7001, Australia
[*]Corresponding author's email: bryana@utas.edu.au

A B S T R A C T

Periglacial processes are active under current climatic conditions on the more exposed peaks and ridges of Tasmania's high country. Non-sorted steps, stripes, and solifluction lobes with vegetated risers and bare treads have formed on many of the mountains capped in fissile sedimentary rocks. Any disturbance to the balance between vegetation and bare ground can result in biogeomorphic feedbacks leading to an increase or decrease in periglacial activity and thereby threaten the survival of fjaeldmark. We tested the hypotheses that vegetation helps create risers by capturing material moved by needle ice, water, and wind, and that the balance between vegetation and bare ground in fjaeldmark is dynamic in Tasmania at the decadal time scale. Repeat photo plots and temperature data loggers were employed to monitor the dynamism of two non-sorted lobes on Mount Rufus over a seven-month period. Diurnal freeze/thaw cycles resulted in needle ice formation on the bare treads and promoted downslope movement of the surface layer through frost creep. Vegetation was observed to reduce geomorphic activity and to capture soil and clasts transported downslope, thereby steepening the risers. Aerial photographic analysis showed a 0.065% per annum increase in vegetation cover in fjaeldmark since the mid-20th century. Mountains that had a high number of days with snow cover were especially prone to increases in vegetation cover. Decline in vegetation cover occurred on some mountains burned during the past century. The smallest changes occurred on the most exposed peaks and ridges.

Introduction

Soil type, moisture availability, slope gradient, freeze/thaw regime, and vegetation type and cover all influence the morphology of landforms that result from solifluction, the genesis of most of which involves permafrost (Washburn, 1979; Matsuoka, 2001; Harris et al., 2008). In marginal periglacial environments like alpine Tasmania, where only the surface layer (typically 5 to 10 cm) freezes, frost creep is the dominant solifluction process (Kiernan, 1985; Slee et al., 2016). This type of solifluction produces shallow landforms, with risers on steps and stripes typically <30 cm tall (Matsuoka, 2001). Solifluction steps have a downslope border composed of bare clasts (sorted) or vegetation (non-sorted). The tread is generally free from vegetation and has a gradient less than that of the general slope of the hillside. Non-sorted steps imperceptibly change into non-sorted stripes at a general slope of approximately 8° (French, 1976; Washburn, 1979).

On mainland Australia, non-sorted steps and lobes have been described from the Mount Kosciuszko region, where they have formed on wind-exposed metasedimentary slopes above 1900 m a.s.l. in a matrix of tall alpine herbfield and fjaeldmark (Costin et al., 1967). On the higher slopes near the mountain crests, radiocarbon analysis of organic materials buried beneath the risers indicate that episodic movement has occurred during the past 300 years. Farther down the slopes, vegetation cover is more complete. Here radiocarbon analysis

yielded ages between 2000 and 3000 yr B.P., suggesting that these steps have not been active for some time (Costin et al., 1967).

In Tasmania, non-sorted lobes, steps, and stripes are common on the summits and ridges of mountains topped with sedimentary rocks, where they typically occur within fjaeldmark (Kirkpatrick and Harwood, 1980; Kirkpatrick, 1984a; Kirkpatrick and Whinam, 1988; Lynch and Kirkpatrick, 1995). The vegetated risers can be dominated by herbs and cushion plants or by shrubs. Interactions between the downslope movement of clasts and soil because of frost creep, redistribution of smaller particles by wind and water, and the capture of clasts and soil by vegetation are postulated to be the primary processes responsible for the formation and persistence of these features (Kirkpatrick and Harwood, 1980; Kirkpatrick, 1984a), some of which are active (Kirkpatrick et al., 2002), and most of which have evidence of activity.

While frost creep, fluvial, and eolian processes are well understood in periglacial environments, the role of vegetation in contributing to the formation of non-sorted stone stripes and steps has been deduced more than demonstrated. Nevertheless, feedbacks between geomorphic processes and vegetation dynamics are known to play an important role in the creation and perseverance of periglacial landforms (Matthews et al., 1998; Eichel et al., 2015).

Succession from active periglacial landforms to inactive ones results from a number of different processes, which cause increased surface stabilization, encouraging the establishment of vegetation (Bryant and Scheinberg, 1970; Haugland, 2006; Hjort, 2014). Needle ice brings larger rocks to the surface and loosens smaller clasts, which get removed by fluvial and eolian processes (French, 1976; Washburn, 1979). As the percentage of fines in the soil decreases, less moisture is retained in the larger rocks, and the formation of needle ice is limited. The increased stability allows lichens, mosses, graminoids, cushion plants, and herbs to begin colonizing the bare ground and encroaching from the boundaries of the tread (Haugland, 2006). Once vegetation cover begins to increase, it offers additional insulation against the more severe freeze/thaw cycles (Luthin and Guymon, 1974), and needle ice growth is suppressed. This biogeomorphic feedback promotes further colonization.

Across the Earth, trees and shrubs have been observed migrating to higher altitudes and latitudes as a response to warmer temperatures and climate change (Harsch et al., 2009; Ernakovich et al., 2014). Fjaeldmark and its associated periglacial landforms have been identified as particularly vulnerable to climate change in Tasmania (Brown, 2009; Visoiu, 2014).

Fjaeldmark vegetation is defined by the mixture of bare ground and vegetated surfaces (Kirkpatrick, 1997) and so can be destroyed by either plant colonization of bare areas or the complete removal of vegetation by geomorphic activity. A decrease in vegetation cover in fjaeldmark was recorded for the Southern Range of Tasmania over the period of a decade in the late 20th century (Kirkpatrick et al., 2002), but the overall pattern of change in fjaeldmark between the mid-20th century and the early 21st century is not known.

Repeat aerial and oblique photography have revealed an expansion of shrubs in arctic tundra (Sturm et al., 2001; Tape et al., 2006), especially after fire (Lantz et al., 2013). A potential positive feedback loop involves the snow-holding capacity of shrubs leading to greater snow accumulation, insulating ground temperatures from the coldest winter months and providing additional moisture that in turn increases soil microbial activity, making more nitrogen available for the shrubs in their summer growing period (Sturm et al., 2005). In Siberia, fjaeldmark and landscapes that contain patterned ground features have been shown to be especially vulnerable to shrub expansion (Frost et al., 2013; Frost and Epstein, 2014). In these environments, bare patches of ground resulting from cryoturbation can offer opportunities for colonization free from the competition of pre-established plant species.

In this paper we test the hypotheses that vegetation creates and reinforces risers by capturing, at the tops of risers, the material moved down the treads by needle ice, water, and wind, and that the balance between vegetation and bare ground in fjaeldmark has been changing in Tasmania at the decadal scale.

Methods

The Study Area

Thirty-eight patches of fjaeldmark from 21 mountains located across Tasmania were used to investigate multidecadal change in the balance between bare ground and vegetation in fjaeldmark (Fig. 1). These sites were selected because of the availability of high-quality and high-resolution historical aerial photographs and the presence of non-sorted steps and stripes. The rocks are predominantly horizontally bedded sandstones, siltstones, and mudstones of the Upper and Lower Parmeener Supergroups (Mineral Resources Tasmania, 2016).

Tasmania has a cool temperate maritime climate that is heavily influenced by prevailing westerly winds. Southwesterly to northwesterly winds frequently exceed 100 km h^{-1} in exposed sites in the alpine zone.

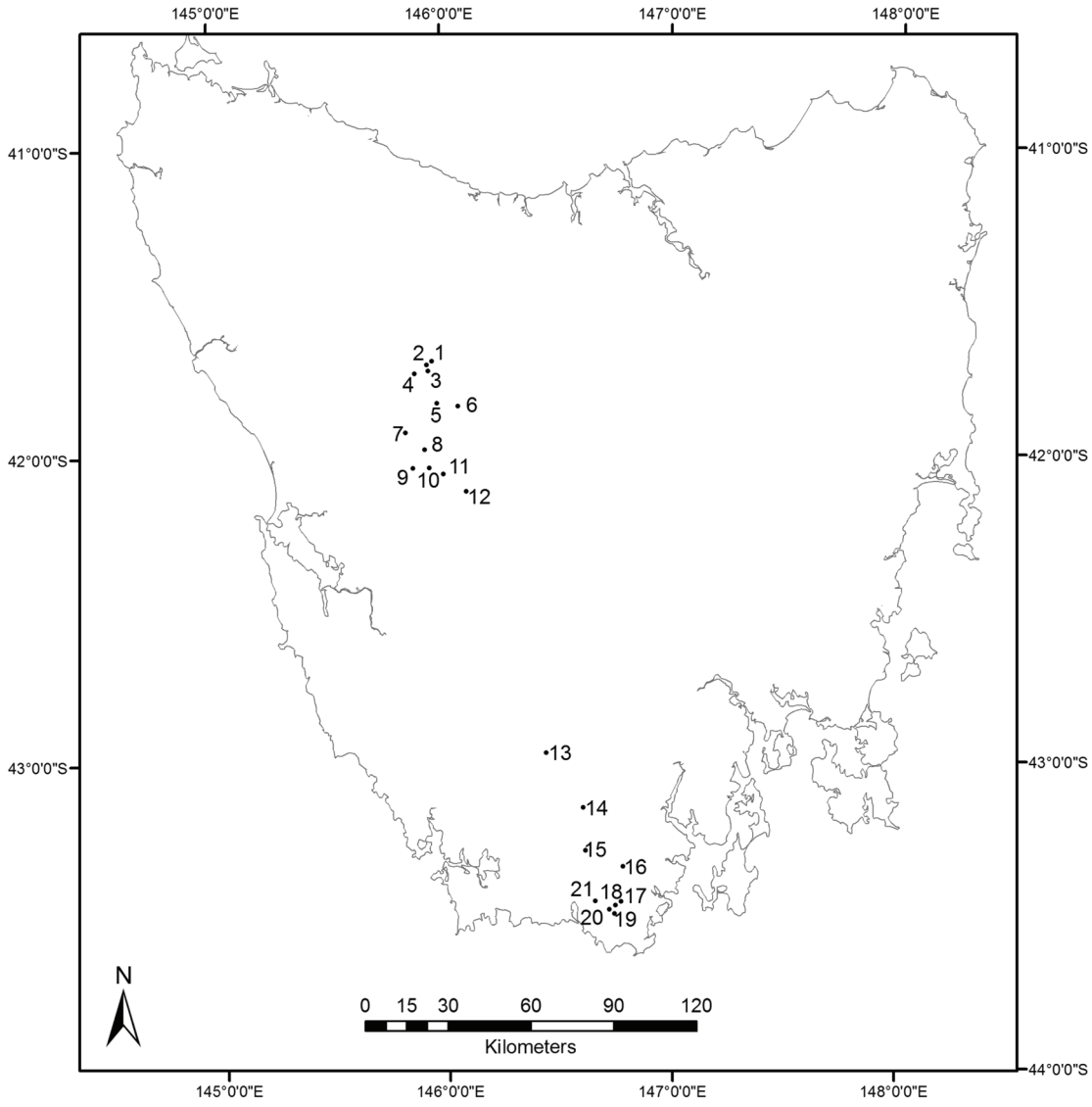

1. Little Mt Emmett (p)	8. High Dome	15. The Boomerang (p)
2. Barn Cirque	9. Rocky Hill (p)	16. Mesa
3. Barn Bluff	10. Pyramid Mountain	17. Hill One (p)
4. Mt Inglis	11. Goulds Sugarloaf	18. Hill Three
5. Mt Pelion West	12. Mt Rufus	19. Mt La Perouse (p)
6. Mt Pelion East	13. Mt Sarah Jane	20. Moonlight Ridge
7. Dome Hill	14. Mt Picton	21. Mt Victoria Cross

FIGURE 1. Location of mountains included in the study, with (p) denoting oblique repeat photo locations (Grid reference: GDA94 MGA Zone 55).

The mean annual precipitation on all the mountains with fjaeldmark exceeds 2500 mm (Nunez et al., 1996). Air temperatures in fjaeldmark in the hottest month approximate a mean of 10 °C, whereas in the coldest month, they approximate 2 °C, resulting in a low persistence of snow cover during winter, except in areas of accumulation on lee slopes.

Mount Rufus (1416 m a.s.l.) is located in central Tasmania (Fig. 2). The surface geology is dominated by fissile Triassic quarzitic sandstones of the Upper Parmeen-

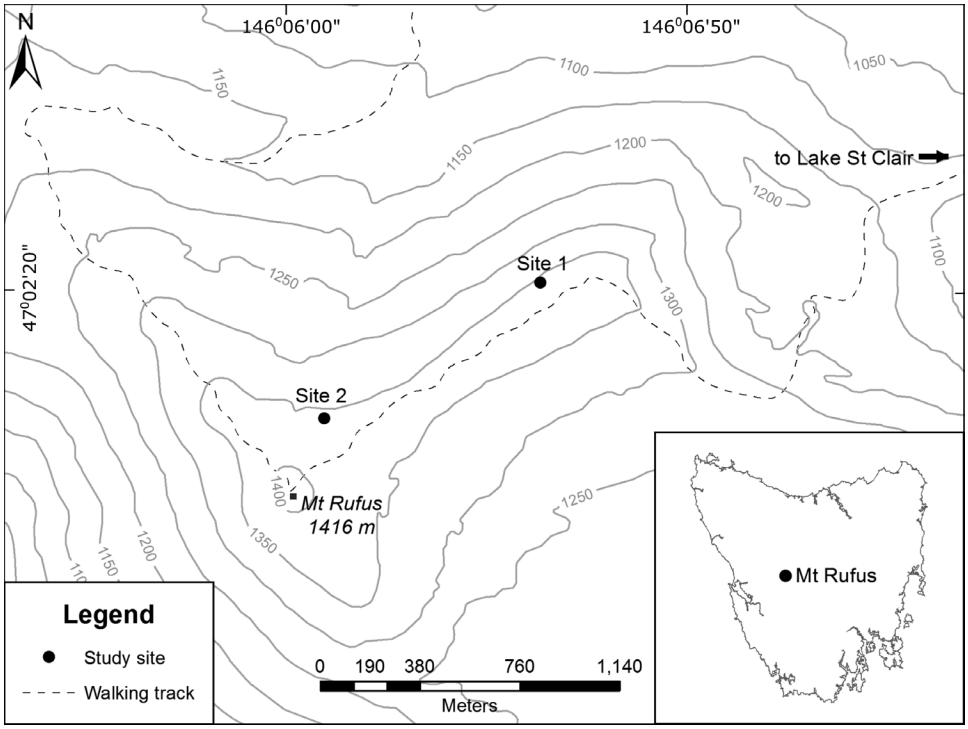

FIGURE 2. Study sites on Mount Rufus.

er Supergroup. On the higher ridges, the sandstone has been thermally hardened upon contact with a dolerite intrusion during the Jurassic (Forsyth, 2003).

Glaciers covered the northern and eastern slopes of Mount Rufus during the last glacial maximum (Derbyshire, 1963; Kiernan, 1985, 1991), and periglacial activity was widespread (Jennings and Mabbutt, 1967; McKinnon et al., 2004). Fires have burned in the alpine areas of Mount Rufus on several occasions in the past century, with the most recent occurring in 1980 (Styger and Balmer, 2009). The climatic treeline at Mount Rufus lies at approximately 1200 m a.s.l. (Harrison-Day et al., 2016), extending up to ~1300 m a.s.l. on the warmer north-facing slopes.

Field Data Collection

Two non-sorted solifluction lobes were selected for short-term observations, both occurring on north-facing slopes on Mount Rufus at an altitude of ~1300 m a.s.l. (Fig. 2). The lobe at Site 1 has a tread approximately 3.6 m wide at its widest point, and is 2.8 m long. The slope of the tread is 11° in the center, with the vegetation covered riser having a slope of 38°. The general slope for the whole site is approximately 25°. The lobe is one of many that extend downslope as a stripe, with channels of active and inactive debris weaving among vegetation. The surface of the bare ground is mainly small stones and pebbles <5 cm along the longest axis, and clayey silt. The occasional larger clast sits on this surface. Where not vegetated, risers have clasts 5 to 25 cm in diameter, and occasionally >25 cm, which trap any downslope movement of fines. Site 2 is a series of non-sorted and sorted solifluction lobes extending downslope in a tongue shape. Bare ground connects all parts of the interior of this feature, and vegetation borders the entirety of its perimeter. It measures 12 m wide at its widest point, and is 38 m long. The general slope for this site is approximately 23°. At the borders of the feature, bare ground terminates in lobate formations banked by vegetation. The vegetated risers vary in steepness from 25° to 45°. The surface sediments are largely the same composition as at Site 1. Steeper slopes generally have larger clasts, rocks, and boulders. Miniature patterned-ground features, including sorted stone polygons (up to 15 cm wide) and sorted stone stripes (up to 1 m long and 15 cm wide), have developed on the bare ground. At the head of the feature, water seeps from between boulders and vegetation.

Near-surface air and ground temperature data were collected hourly from 9 September 2015 to 13 April 2016 using Tinytag Plus 2 TGO-4017 temperature data loggers (Gemini Data Loggers Ltd., 2014). Data loggers buried 5 cm below the surface recorded ground temperature, with the loggers attached to a wooden stake by a short length of thin wire to assist in relocation.

Near surface air temperatures were recorded 5 cm above the surface, with the data loggers attached to the same wooden stakes. A radiation shield constructed of PVC pipe 10 cm tall × 8 cm in diameter, with a number of holes perforating the sides, was used. At each of the 2 sites, a data logger pair (measuring both air and ground temperatures) was installed in the center of the bare tread of the solifluction lobe, and another pair inside *Orites revolutus* R.Br. shrubs on the risers.

Twenty-five photo plots were marked out and photographed on 13 September 2015. They were concentrated on the boundaries between bare and vegetated ground. A 1 m × 1 m quadrat made from 20 mm conduit was used to delineate the perimeter of each plot. All plots were relocated and photographed again on 13 April 2016.

A series of time lapse photographs was used to capture a single freeze/thaw event over the night of 21 September 2015 (https://youtu.be/Rb4SDon8OG4). A GoPro HERO3 White action camera coupled with a CamDo time lapse intervalometer (CamDo Solutions, 2016) was mounted on a tripod and set to take a photograph every 45 min for a time period of 18 h. A neoprene cover was constructed and fastened over the camera to insulate it against subzero temperatures. The site was kept illuminated by a small LED light.

An assemblage of historic vertical and oblique photographs depicting Tasmanian fjaeldmark was obtained from private collections. The oblique scenes were rephotographed between September 2015 and February 2016, with the period of time elapsing between the original photographs and the repeat photographs varying between 26 and 44 years.

Photographic Processing

Photographs of the 1 × 1 m quadrats on Mount Rufus were corrected for geometric distortion using the program Adobe Photoshop CS6. Stratified random sampling was used to select up to 25 clasts from each quadrat. A grid with 25 equally spaced squares with a point placed randomly in each cell was overlaid on the image. The visible surface area of the clast that was directly below the point on the latest photograph was measured. In the case of no visible clasts being directly below the point, or the clast not being identifiable in each of the photographic pairs, the nearest clast that was identifiable in both photographs was selected. Any clast movement in the second image from the original position in the first image was measured using a straight line drawn from the center. The visible surface area of each selected clast and the direction and degree of movement were recorded. The scale of each image was set using the bottom edge of the quadrat. The program ImageJ (Schneider et al., 2012) was used for all clast movement measurements.

The historical aerial photographs were compared with Tasmania's Orthophoto mosaic (DPIPWE, 2016a), available as a free base layer on ArcGIS 10.3 (ESRI, 2014). The metadata for each photograph used in this mosaic were obtained from the Aerial Photo Viewer (DPIPWE, 2016b). The time period between successive vertical aerial photographs of the same places varied from 26 years to 59 years.

The total extent of fjaeldmark was outlined with a polygon on the most recent photographs. Images were displayed side by side on the computer monitor, with any increase or decrease in vegetation cover marked onto the newer photograph with a polygon.

The total fjaeldmark area and any increase or decrease in vegetation cover were measured for areas above and below the treeline, on north- and south-facing slopes, and on slopes >8° and <8°. The climatic treelines were determined by carefully examining the maximum altitude of trees on each mountain on the latest aerial photographs. Where available in the literature (Kirkpatrick and Harwood, 1980; Kirkpatrick, 1982; Kirkpatrick and Balmer, 1991), previously observed treelines were used. A digital elevation model (DEM) was created using the 10 m contour lines available from the LIST (DPIPWE, 2016a) and the Topo to Raster tool in ArcGIS. Slope was then calculated using the Slope tool, with slopes divided into either >8° or <8° using the Raster Calculator tool. The Aspect tool was used to calculate aspect, with the Reclassify tool used to define either north- or south-facing slopes.

The geometric area (m^2) of all polygons was calculated using the Calculate Geometry tool in the attributes table. Results were exported to Microsoft Excel, with the net annual percentage change in vegetation cover being calculated for each site.

Data Analysis

All data analysis was carried out in Minitab 17 Statistical Software (2010). The Kruskal-Wallis H Test was used to determine if any changes in vegetation cover above or below the treeline, on north- or south-facing slopes, or on slopes greater or less than 8°, affected the total change in vegetation cover. Each site was grouped into either northern (north of Mount Sarah Jane) or southern (south of, and including, Mount Sarah Jane) fjaeldmark patches. Difference in the net annual percentage change in vegetation between the two groups was tested for using the Kruskal-Wallis H Test. The percentage of clear days that the highest point of each mountain had snow cover for the years 1983 to 2013

(inclusive) (Kirkpatrick, et al., 2017), and increase in the percentage of clear days with snow cover over this time period (personal communication from Kirkpatrick to Annandale, June 2016) were correlated with the net annual percentage change in vegetation cover.

Results and Discussion

Short-Term Observations

There were 54 (Site 1) and 53 (Site 2) freeze/thaw cycles on the unvegetated treads of the solifluction lobes on Mount Rufus over the 216 days of temperature recordings. In the vegetated risers, 47 (Site 1) and 41 (Site 2) freeze/thaw cycles occurred. The coldest air temperature on the unvegetated treads was –6.8 °C, and on the vegetated risers –3 °C. At no time did temperatures 5 cm below the surface drop below 0 °C, confirming that needle ice is the primary agent of cryoturbation. In winter, periodic shallow ground freezing may facilitate gelifluction (Slee et al., 2015), but the limited temporal extent of such freezing would limit its effectiveness as an agent for downslope mass movement.

The vegetated risers had warmer minimum air temperatures than the unvegetated treads (Site 1: paired $t = -6.38$, $P < 0.001$; Site 2: paired $t = -9.9$, $P < 0.001$). Maximum air temperatures were greater on the vegetated risers than on the unvegetated treads at Site 1 (paired $t = -8.69$, $P < 0.001$), but at Site 2 the converse was true (paired $t = 17.97$, $P < 0.001$). Site 2 had thicker vegetation cover, thereby reducing insolation; whereas, at Site 1, vegetation cover was sparser. Also, the vegetation situated upslope of the data logger at Site 1 may have trapped outgoing radiation, creating a "solar oven" effect. Minimum ground temperatures did not differ significantly between vegetated and unvegetated sites (Site 1: paired $t = 0.8$, $P = 0.426$; Site 2: paired $t = 0.29$, $P = 0.771$), while maximum ground temperatures were higher on the treads (Site 1: paired $t = 19.63$, $P < 0.001$; Site 2: paired $t = 21.37$, $P < 0.001$).

In the repeat photo quadrats, the difficulty in re-identifying small clasts lead to a bias toward measuring larger clasts. Only 20 (3.9%) of clasts measured were less than 1 cm^2. The median area of the 510 clasts measured was 5.6 cm^2, and the median displacement was 1.96 cm. The mean size of clasts that moved was 9.3 cm^2 and was smaller than the mean size of clasts that did not move (mean = 29 cm^2) ($t = -4.8$, df = 302, $P < 0.001$). The steepness of slope did not have an effect on whether a clast moved or did not move. Clasts were more likely to move downslope than across or upslope ($H = 11.5$, df = 1, $P = 0.001$). Slope did not have any effect on whether a clast became more buried by sediments, more exposed, or exhibited no change at all.

The study site was visited on 12–13 and 21–22 October 2015, and 12–13 April 2016, with overnight minimum air temperatures on the unvegetated tread of Site 2 reaching 1.3 °C, –2.9 °C, and 0.4 °C, respectively. Only on the night of 21 October 2015 did needle ice develop. On this evening, minimum air temperatures reached –2.4 °C in the vegetated riser. Visible needle ice formation began at 21:31 hours when air temperatures were –1.3 °C. The ice continued to grow until 05:56 hours the following morning (temperature = –2.2 °C). Melting began at 06:41 hours (temperature = –1.5 °C), with all visible ice melted by 08:54 hours (temperature = 2.6 °C).

Measurements taken from a marker pen located in the center of the image indicate that the height of the needle ice was approximately 16 mm, with lifted material moving 10 mm downslope following thawing. The observed downslope movement of clasts lifted by needle ice can be compared with the theoretical movement estimated with the equation:

$$D = h \tan(\Theta), \quad (1)$$

where D = downslope displacement in mm, h = height of needle ice in mm, and Θ = slope in degrees. Using the measurements of the pen from the time lapse photography, with a slope of 23°, an estimate of 6.8 mm of downslope movement was calculated. This equation assumes that as the needle ice melts, the clast drops vertically to the surface. Through laboratory experiments, Higashi and Corte (1971) found that as the needle ice melted, clasts fell, rolled, and slid downslope instead of dropping vertically and settling. They formulated the equation:

$$D = C\, h \tan(\Theta)^2, \quad (2)$$

where C is a constant representing the stochastic movement of clasts due to toppling, rolling, and bending needle ice. Using this equation and C = 3 (Matsuoka, 1998), downslope movement is estimated to be 8.7 mm. Through observations in the field, Mackay and Mathews (1974) estimated that downslope movement was close to the height of needle ice growth:

$$D = h. \quad (3)$$

This would estimate downslope movement to be approximately 16 mm. From these three different models, that of Higashi and Corte (1971) best matches the 10 mm of downslope movement measured from the marker pen in the time lapse photographs. Matsuoka (1998) also found that Equation (2) best predicted downslope movement in his study on frost creep in the Japanese Alps.

Miniature patterned ground features, including sorted stone stripes and sorted stone polygons, were observed forming on the treads. Over the seven-month observation period, there was a noted removal or buildup of fine materials around larger rocks. This is consistent with the outcomes of fluvial processes, with the direction of sediment movement being downslope.

Vegetation was observed acting in a number of ways to slow the downslope movement of materials. Around the upper borders of the vegetated risers, clasts that had been moving downslope were trapped by the vegetation. Over the summer the vegetation stabilized captured clasts within its branches (Fig. 3). The increased vegetation cover is likely to allow more clasts to be captured as they move downslope. The addition of rocks and soils into the vegetated risers provides extra substrate for the vegetation, allowing these risers to slowly increase in height. If downslope surface movement exceeds the ability for vegetation to capture the clasts, then the vegetation will be overrun, forming a "blow out" on the riser (Fig. 4).

The same freeze/thaw witnessed on 21 October 2015 saw extensive fields of needle ice develop on patches of bare ground. Ground beneath vegetation was largely free of ice (Fig. 5). A small *Orites revolutus* R.Br. plant was observed holding back clasts lifted by needle ice (Fig. 6), among many other instances of the same phenomenon. The vegetation of the risers was dominated by *O. revolutus*, *Richea sprengeloides* F.Muell., *Epacris serpyllifolia* R.Br., and *Baeckea gunniana* Schauer, with an understory that included *Exocarpos humifusus* R.Br., *Schizacme montana* Hook.f., *Poa* sp., and several species of mosses and lichens. *Tasmannia lanceolata* Poir, *Planocarpa petsolaris* C.M.Weiller, *Olearia algida* N.A.Wakef., *Ozothamnus ledifolius* Hook.f., and *Coprosma nitida* Hook.f. were also present. Some of these species vegetatively reproduce (Kirkpatrick, 1984b), a trait that may assist in their perseverance in this geomorphically active environment.

Decadal Change

Forty-six percent of the 382 ha of fjaeldmark that were mapped occurred above the climatic treeline. Slopes <8° had 22% of the 382 ha, and north-facing slopes had 41% (Table 1). There was an overall mean increase in vegetation cover of 0.065% per annum. The fjaeldmark on the ridge extending to the south of Mount Pelion West had the greatest increase (Table 2). Here the fjaeldmark was all below the climatic treeline, faced north and was predominantly on a slope <8°. The summit area of Rocky Hill had the greatest decrease (Table 2), most likely because of erosion on the steeper west-facing slopes following the fire that burned through the area in 1934. There was no difference in the annual percentage of vegetation cover change between those areas measured above and below the treeline, on north- and south-facing slopes, and on slopes greater or less than 8°. The smallest changes occurred on the most exposed locations, such as mountain summits, where desiccating hot winds and limited water availability in summer, and abrasive ice laden winds and cold temperatures in winter limit plant growth.

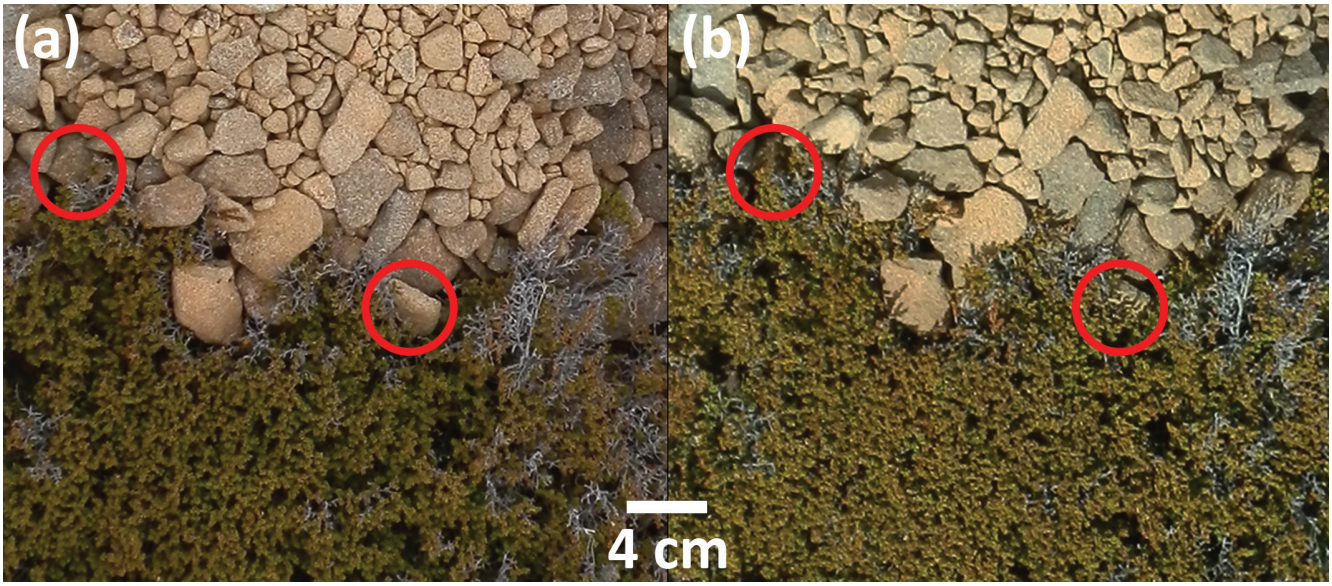

FIGURE 3. ***Baeckea gunniana*** **Schauer stabilizing clasts at the top of a riser over a seven-month period. Photograph (a) taken on 13 September 2015, and photograph (b) taken on 13 April 2016.**

FIGURE 4. An overflow of sediment on a vegetated riser composed primarily of *Planocarpa petiolaris* C.M.Weiller at the bottom of a non-sorted stripe on Little Mount Emmett. Photo taken 25 September 2015. For scale, camera case is 12 cm long.

FIGURE 5. Needle ice on tread, but absent under vegetation. For scale, pen is 16 cm long.

The repeat oblique photography reinforced the results of the aerial photograph analysis, with incidences of increasing vegetation cover exceeding incidences of vegetation loss (Fig. 7). With the exception of Hill One, the locations of the treads and risers of the non-sorted steps have not changed, and most individual rocks are located in the same positions that they were decades ago. Some individual shrubs of *Leptospermum rupestre* Hook.f., *Richea scoparia* Hook.f., *Athrotaxis selaginoides* D.Don, and *Diselma archeri* Hook.f. increased in size to cover some of the previously bare ground. Ongoing erosion, and dieback of individual shrubs, provided incidences of vegetation retreat (Fig. 7).

Vegetation increased behind rocks and pre-existing vegetation to the leeward side of the prevailing westerly winds. As vegetation cover in fjaeldmark continues to increase, the number of protected sites may also increase, offering further opportunity for plant establishment. This positive feedback loop could lead to an accelerated increase in vegetation cover in the absence of any disturbance events, and a shift in community structure from fjaeldmark to vegetation with complete cover.

Vegetation cover change increased with snow incidence ($r = 0.400$, df = 36, $P = 0.012$) and change in snow incidence ($r = 0.361$, df = 36, $P = 0.026$), perhaps reflecting the efficacy of snow in protection from the ice-laden abrasive winds and intense freeze/thaw cycles of winter (McVean, 1958; Billings and Bliss, 1959; Körner, 1999).

FIGURE 6. Capture of frost-displaced clasts by riser vegetation.

The northern mountains had a greater annual percentage change in vegetation cover than the southern mountains, with a median increase of 0.041% per annum compared to 0.001% per annum in the south ($H = 4.94$, $df = 1$, $P = 0.026$). The northern mountains are the greatest distance from the southwest coast, and thus have a more continental climate than the southern mountains, making the persistence of winter snow more likely.

A lack of disturbance events could also be influencing the encroachment of vegetation. Rocky Hill, burned in 1934 (Kirkpatrick, 1984a), had a decrease in vegetation cover, most likely triggered by slope instability following fire. However, the less exposed fjaeldmark around Barn Bluff and above Cradle Cirque has been burned in the late 1800s or early 1900s (Kirkpatrick and Balmer, 1991) and had a strong increase in vegetation cover. Fire can remove vegetation and reactivate geomorphic activity (Kirkpatrick, 1984a; Shakesby and Doerr, 2006; Sass et al., 2012). On the southern slope of Rocky Hill South, fluvial erosion has revealed a section of *Athrotaxis* log previously buried beneath the fjaeldmark. Kirkpatrick (1984a) suggested that the hill may have been forested in the past, with fire killing the *Athrotaxis* and the following period of instability resulting in its burial. While this hypothesis cannot be excluded, other *Athrotaxis* logs displaying similar wind-abraded surfaces have been observed surviving as krummholtz in the fjaeldmark of the Boomerang. This suggests that a forest may not have been necessary for the Rocky Hill South log to have grown to that size, and that *Athrotaxis* trees may have existed there as krummholtz among the fjaeldmark for long periods of time.

The 530 m^2 increase of vegetation cover at Hill One over 59 years is opposite to the vegetation loss in the 11 years after 1989 recorded by Kirkpatrick et al. (2002) and indicated for a longer recent period by Figure 7. It is possible that there was a general trend in increasing vegetation cover until the 1980s, with the years 1989 to 2016 experiencing a period of increased erosion and fjaeldmark expansion, perhaps as a result of the strengthening winds caused by a steepening of atmospheric pressure gradients resulting from climate change (Kirkpatrick et al., 2017).

Conclusions

The non-sorted solifluction lobes of Mount Rufus are active under current climatic conditions. The absence of ground freezing and subsequent dominance of diurnal freeze/thaw processes driving periglacial activity confirms the previous conclusion of Slee et al. (2016) that the area is only marginally periglacial. Periglacial and fluvial processes were the main contributors to downslope surface movement.

Vegetation reduces downslope movement by creating a thermal barrier limiting the development of needle ice, holding back clasts lifted by needle ice from moving downslope, capturing clasts transported downslope by either fluvial or periglacial processes, and stabilizing the risers. A positive feedback builds up the riser and gives form to the non-sorted solifluction lobe.

Vegetation cover has been increasing in fjaeldmark on net. While some areas containing fjaeldmark and periglacial features appear to be stable at present, others are dynamic. In the absence of fire or other disturbance

TABLE 1

Total area (ha) of fjaeldmark by mountain and its geographical distribution depending on aspect, slope, and location of the climatic treeline.

Mountain	Total area	Above treeline	Below treeline	Slope < 8°	Slope > 8°	North-facing	South-facing
The Boomerang	31.78	16.29	15.49	7.43	24.35	16.51	15.27
Barn Bluff	3.01	0.00	3.01	1.90	1.11	0.97	2.04
Mesa	1.43	0.00	1.43	0.66	0.77	1.15	0.27
Mount Sarah Jane	2.38	0.12	2.26	0.91	1.46	0.26	2.12
Mount Pelion East	8.43	8.43	0.00	1.32	7.11	3.01	5.43
Mount Pelion West a	0.55	0.00	0.55	0.14	0.41	0.55	0.00
Mount Pelion West b	5.71	0.41	5.30	0.00	5.71	0.00	5.71
Mount Pelion West c	1.15	0.00	1.15	0.00	1.15	0.00	1.15
Mount Pelion West d	3.23	0.00	3.23	0.00	3.23	0.00	3.23
Mount Picton a	2.45	0.73	1.73	2.03	0.42	1.21	1.24
Mount Picton b	2.75	0.00	2.75	0.83	1.92	1.27	1.48
Mount Chapman	0.32	0.00	0.32	0.00	0.32	0.00	0.32
Mount Inglis	35.80	3.54	32.26	7.20	28.60	14.55	21.25
Bluff Cirque	2.26	2.00	0.26	0.29	1.97	1.82	0.45
Cradle Cirque	0.94	0.00	0.94	0.64	0.30	0.41	0.53
Little Mount Emmett	8.86	0.00	8.86	0.36	8.50	3.29	5.57
Dome Hill	46.76	0.00	46.76	11.57	35.19	16.98	29.78
High Dome W	6.14	0.00	6.14	0.24	5.90	3.04	3.10
The Amphitheatre	3.37	0.00	3.37	0.00	3.37	0.89	2.47
Rocky Hill south	4.67	0.00	4.67	2.62	2.05	1.84	2.83
Rocky Hill main	13.86	0.00	13.86	1.08	12.78	4.92	8.95
Rocky Hill east	1.96	0.00	1.96	0.07	1.89	0.83	1.13
Pyramid Mountain a	10.23	0.00	10.23	0.97	9.26	3.89	6.34
Pyramid Mountain b	5.40	0.00	5.40	3.38	2.02	2.27	3.13
Gould's Sugarloaf	12.43	8.01	4.42	0.00	12.43	1.18	11.24
Little Sugarloaf	10.00	8.18	1.82	0.61	9.39	4.51	5.48
Mount Victoria Cross	12.28	2.76	11.68	3.43	8.85	3.55	8.72
Mount Wylly	6.48	2.53	3.95	0.67	5.81	1.24	5.24
Table Top	6.32	4.60	1.73	3.72	2.61	2.55	3.78
Hill One	7.32	6.51	0.81	0.57	6.75	2.59	4.73
Hill Two	11.09	11.09	0.00	3.61	7.49	4.80	6.29
Hill Three	8.77	8.64	0.13	1.92	6.85	4.45	4.32
Hill Four	12.83	10.24	2.59	2.95	9.89	4.46	8.37
Agnetes Garden	6.57	0.00	6.57	2.22	4.35	1.65	4.92
Maxwell Ridge	31.42	30.95	0.47	8.07	23.35	14.33	17.10
Mount La Perouse a	10.88	10.88	0.00	4.17	6.70	5.32	5.56
Mount La Perouse b	35.65	35.65	0.00	7.43	28.22	20.79	14.86
Mount Rufus	6.43	6.40	0.04	0.05	6.38	4.63	1.80

TABLE 2

Change in vegetation cover per year, as a percentage of the total area of fjaeldmark; negative values indicate a decrease in vegetation cover.

Mountain	Total	Above treeline	Below treeline	Slope <8°	Slope >8°	North-facing	South-facing
The Boomerang	0.019	0.014	0.006	0.026	0.017	0.016	0.022
Barn Bluff	0.381	*	0.381	0.120	0.829	0.818	0.173
Mesa	0.131	*	0.131	0.045	0.205	0.125	0.158
Mount Sarah Jane	0.014	0.000	0.016	0.009	0.017	0.006	0.015
Mount Pelion East	0.021	0.021	*	0.000	0.025	0.019	0.030
Mount Pelion West a	0.398	*	0.398	1.001	0.186	0.398	*
Mount Pelion West b	0.081	0.159	0.075	*	0.081	*	0.081
Mount Pelion West c	0.209	*	0.209	*	0.209	*	0.209
Mount Pelion West d	0.083	*	0.083	*	0.083	*	0.083
Mount Picton a	0.336	0.423	0.300	0.361	0.217	0.458	0.218
Mount Picton b	0.281	*	0.281	0.285	0.280	0.321	0.247
Mount Chapman	0.000	*	0.000	*	0.000	*	0.000
Mount Inglis	0.036	0.108	0.028	0.012	0.042	0.030	0.040
Bluff Cirque	0.011	0.009	0.025	0.003	0.012	0.004	0.039
Cradle Cirque	0.042	*	0.042	0.024	0.079	0.035	0.047
Little Mount Emmett	0.040	*	0.040	0.012	0.041	0.077	0.018
Dome Hill	0.057	*	0.057	0.071	0.052	0.088	0.039
High Dome W	0.071	*	0.071	0.000	0.074	0.120	0.023
The Amphitheatre	0.075	*	0.075	*	0.075	0.059	0.081
Rocky Hill south	0.005	*	0.005	0.003	0.008	0.000	0.008
Rocky Hill main	-0.027	*	-0.027	-0.044	-0.026	0.017	-0.051
Rocky Hill east	0.005	*	0.005	0.145	0.000	0.013	0.000
Pyramid Mountain a	0.029	*	0.029	0.002	0.032	0.073	0.002
Pyramid Mountain b	0.004	*	0.004	0.006	0.000	0.008	0.000
Gould's Sugarloaf	0.023	0.009	0.048	*	0.023	0.052	0.020
Little Sugarloaf	0.077	0.044	0.226	0.063	0.078	0.059	0.092
Mount Victoria Cross	-0.006	0.000	-0.006	0.001	-0.008	0.001	-0.008
Mount Wylly	0.006	-0.017	0.022	0.032	0.003	0.000	0.008
Table Top	0.002	0.000	0.006	0.001	0.002	0.003	0.001
Hill One	0.013	0.000	0.111	0.000	0.014	0.019	0.009
Hill Two	0.008	0.008	*	0.006	0.009	0.001	0.013
Hill Three	0.009	0.008	0.085	0.003	0.010	0.012	0.005
Hill Four	0.003	-0.001	0.017	0.005	0.003	0.007	0.001
Agnetes Garden	0.023	*	0.023	0.023	0.023	0.043	0.016
Maxwell Ridge	0.006	0.005	0.050	0.001	0.008	0.010	0.003
Mount La Perouse a	0.005	0.005	*	0.007	0.004	0.008	0.003
Mount La Perouse b	0.001	0.001	0.000	0.000	0.002	0.002	0.000
Mount Rufus	0.014	0.015	0.000	0.142	0.013	0.013	0.019

* = none in class.

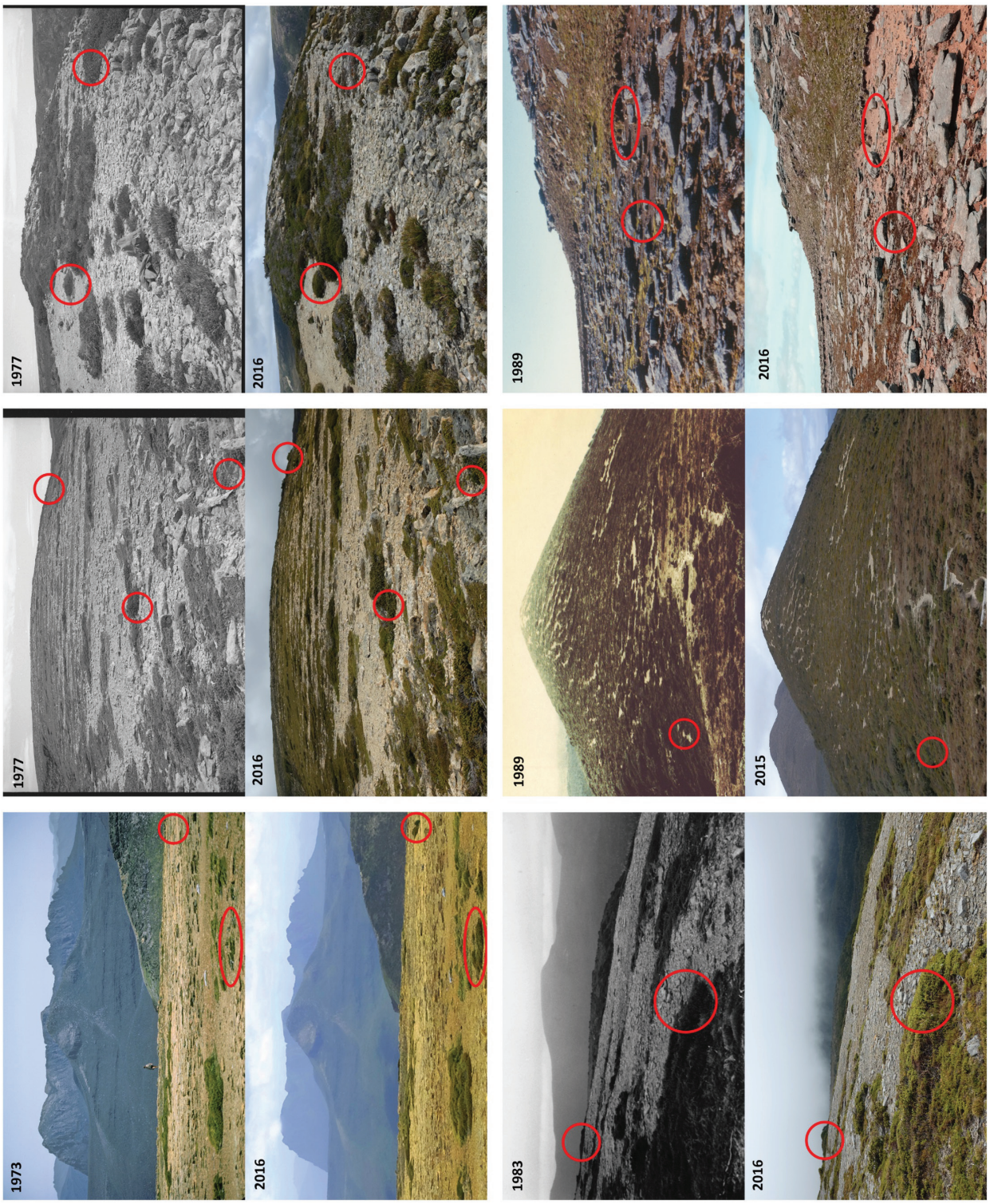

FIGURE 7. Repeat photographic pairs with year of photo given. Top left is Mount La Perouse, top middle and right is The Boomerang, bottom left is Rocky Hill, bottom middle is Little Mount Emmett, bottom right is Hill One.

events, fjaeldmark and its associated active periglacial features may diminish in Tasmania, with heath taking its place. Exceptions to this may occur in the more exposed and extreme environments, where fjaeldmark and periglacial landforms may be able to persist over the next tens to hundreds of years.

Acknowledgments

We would like to thank the Department of Primary Industry, Parks, Water and Environment, Tasmania, for field permits, and Violet Harrison-Day for assistance with field work. Thanks also to Anolia Jasmyn Jayn

Lynch and Dennis Garrett for the use of their photographs in this publication.

References Cited

Billings, W. D., and Bliss, L. C., 1959: An alpine snowbank environment and its effects on vegetation, plant development, and productivity. *Ecology*, 40: 388–397.

Brown, M. J., 2009: *Monitoring the Impact of Climate Change on the Flora and Vegetation Values of the Tasmanian Wilderness World Heritage Area: a Review.* Hobart: Department of Primary Industry, Parks, Water and Environment, unpublished report, http://dpipwe.tas.gov.au/Documents/Impact-of-Climate-Change-on-the-WWHA.pdf, accessed 20 February 2016.

Bryant, J. P., and Scheinberg, E., 1970: Vegetation and frost activity in an alpine fellfield on the summit of Plateau Mountain, Alberta. *Canadian Journal of Botany*, 48: 751–771.

CamDo Solutions, 2016: *Time lapse intervelometer*, http://camdo.com/collections/long-term-time-lapse/products/time-lapse-intervalometer, accessed 16 March 2016.

Costin, A. B., Thom, B. G., Wimbush, D. J., and Stuiver, M., 1967: Nonsorted steps in the Mt. Kosciusko area, Australia. *Geological Society of America Bulletin*, 78: 979–992.

Derbyshire, E., 1963: Glaciation of the Lake St. Clair district, west-central Tasmania. *The Australian Geographer*, 9: 97–110.

DPIPWE [Department of Primary Industry, Parks, Water and Environment], 2016a: LISTmap, http://maps.thelist.tas.gov.au/listmap/app/list/map, accessed 10 February 2016.

DPIPWE [Department of Primary Industry, Parks, Water and Environment], 2016b: Aerial Photo Viewer, https://www.thelist.tas.gov.au/app/content/the-list/aerialphotoviewer/, accessed 10 February 2016.

Eichel, J., Corenblit, D., and Dikau, R., 2015: Conditions for feedbacks between geomorphic and vegetation dynamics on lateral moraine slopes: a biogeomorphic feedback window. *Earth Surface Processes and Landforms,* 41: 406–419.

Ernakovich, J. G., Hopping, K. A., Berdanier, A. B., Simpson, R. T., Kachergis, E. J., Steltzer, H., and Wallenstein, M. D., 2014: Predicted responses of arctic and alpine ecosystems to altered seasonality under climate change. *Global Change Biology*, 20: 3256–3269.

ESRI, 2014: ArcGIS Desktop: Release 10.3. Redlands, California: Environmental Systems Research Institute.

Forsyth, S., 2003: Geology of the Mount Koonya area. Hobart: Department of Infrastructure, Energy and Resources, *Tasmanian Geological Survey Record 2003/08*: 31 pp.

French, H. M., 1976: *The Periglacial Environment*. London: Longman Group Limited, 309 pp.

Frost, G. V., and Epstein, H. E., 2014: Tall shrub and tree expansion in Siberian tundra ecotones since the 1960s. *Global Change Biology*, 20: 1264–1277.

Frost, G. V., Epstein, H. E., Walker, D. A., Matyshak, G., and Ermokhina, K., 2013: Patterned-ground facilitates shrub expansion in Low Arctic tundra. *Environmental Research Letters*, 8(1): 015035, doi: https://dx.doi.org/10.1088/1748-9326/8/1/015035.

Gemini Data Loggers Ltd., 2014: *Tinytag Plus 2 Data Sheet*, http://gemini2.assets.d3r.com/pdfs/original/1584-tgp-4017.pdf, accessed 16 March 2016.

Harris, C., Kern-Luetschg, M., Murton, J., Font, M., Davies, M., and Smith, F., 2008: Solifluction processes on permafrost and non-permafrost slopes: results of a large-scale laboratory simulation. *Permafrost and Periglacial Processes*, 19(4): 359–378.

Harrison-Day, V., Annandale, B., Balmer, J., and Kirkpatrick, J. B., 2016: The influence of climate change and fire on alpine treeless vegetation at Mount Rufus, Tasmania. Unpublished manuscript, University of Tasmania, Hobart.

Harsch, M. A., Hulme, P. E., McGlone, M. S., and Duncan, R. P., 2009: Are treelines advancing? A global meta-analysis of treeline response to climate warming. *Ecology Letters*, 12: 1040–1049.

Haugland, J. E., 2006: Short-term periglacial processes, vegetation succession, and soil development within sorted patterned ground: Jotunheimen, Norway. *Arctic, Antarctic, and Alpine Research*, 38: 82–89.

Higashi, A., and Corte, A. E., 1971: Solifluction: a model experiment. *Science*, 171: 480–482.

Hjort, J., 2014: Which environmental factors determine recent cryoturbation and solifluction activity in a subarctic landscape? A comparison between active and inactive features. *Permafrost and Periglacial Processes*, 25: 136–143.

Jennings, J. N., and Mabbutt, J. A., 1967: *Landform Studies from Australia and New Guinea*. Canberra: Australian National University Press, 434 pp.

Kiernan, K., 1985: *Late Cainozoic Glaciation and Mountain Geomorphology in the Central Highlands of Tasmania*. Ph.D. thesis, University of Tasmania, Hobart.

Kiernan, K., 1991: Glacial history of the upper Derwent Valley, Tasmania. *New Zealand Journal of Geology and Geophysics*, 34: 157–166.

Kirkpatrick, J. B., 1982: Phytogeographical analysis of Tasmanian alpine floras. *Journal of Biogeography*, 9: 255–271.

Kirkpatrick, J. B., 1984a: Tasmanian high mountain vegetation II—Rocky Hill and Pyramid Mountain. *Papers and Proceedings of the Royal Society of Tasmania,* 118: 5–20.

Kirkpatrick, J. B., 1984b: Altitudinal and successional variation in the vegetation of the West Coast Range, Tasmania. *Australian Journal of Ecology,* 9: 81–91.

Kirkpatrick, J. B., 1997: *Alpine Tasmania: an Illustrated Guide to the Flora and Vegetation*. Melbourne: Oxford University Press, 196 pp.

Kirkpatrick, J. B., and Balmer, J., 1991: The vegetation and higher plant flora of the Cradle Mountain–Pencil Pine area, northern Tasmania. *In* Banks, M. R., Smoth, S. J., Orchard, A. E., and Kantvilas, G. (eds.), *Aspects of Tasmanian Botany*. Hobart: Royal Society of Tasmania, 119–148.

Kirkpatrick, J. B., and Harwood, C. E., 1980: Vegetation of an infrequently burned Tasmanian mountain region. *Proceedings of the Royal Society of Victoria*, 91: 79–107.

Kirkpatrick, J. B., and Whinam, J., 1988: Tasmanian high mountain vegetation: 3. Lake Ewart, Dome Hill and Eldon Bluff. *Papers and Proceedings of the Royal Society of Tasmania,* 122: 145–164.

Kirkpatrick, J. B., Bridle, K. L., and Lynch, A. J. J., 2002: Changes in alpine vegetation related to geomorphological processes and climatic change on Hill One, Southern Range, Tasmania, 1989–2000. *Australian Journal of Botany*, 50: 753–759.

Kirkpatrick, J. B., Nunez, M., Bridle, K. L., Parry, J., and Gibson, N., 2017: Causes and consequences of variation in snow incidence on the high mountains of Tasmania, 1983–2013. *Australian Journal of Botany*, 64: doi: https://dx.doi.org/10.1071/BT16179.

Körner, C., 1999: *Alpine Plant Life: Functional Plant Ecology of High Mountain Ecosystems*. Berlin: Springer Verlag, 349 pp.

Lantz, T. C., Marsh, P., and Kokelj, S. V., 2013: Recent shrub proliferation in the Mackenzie Delta uplands and microclimatic implications. *Ecosystems*, 16: 47–59.

Luthin, J. N., and Guymon, G. L., 1974: Soil moisture-vegetation-temperature relationships in central Alaska. *Journal of Hydrology*, 23: 233–246.

Lynch, A. J. J., and Kirkpatrick, J. B., 1995: Pattern and process in alpine vegetation and landforms at Hill One, Southern Range, Tasmania. *Australian Journal of Botany*, 43: 537–554.

Mackay, J. R., and Mathews, W. H., 1974: Movement of sorted stripes, the Cinder Cone, Garibaldi Park, BC, Canada. *Arctic and Alpine Research*, 6: 347–359.

Matsuoka, N., 1998: The relationship between frost heave and downslope soil movement: field measurements in the Japanese Alps. *Permafrost and Periglacial Processes*, 9: 121–133.

Matsuoka, N., 2001: Solifluction rates, processes and landforms: a global review. *Earth-Science Reviews*, 55: 107–134.

Matthews, J. A., Shakesby, R. A., Berrisford, M. S., and McEwen, L., 1998: Periglacial patterned ground on the Styggedalsbreen glacier foreland, Jotunheimen, southern Norway: micro-topographic, paraglacial and geoecological controls. *Permafrost and Periglacial Processes*, 9: 147–166.

McKinnon, G. E., Jordan, G. J., Vaillancourt, R. E., Steane, D. A., and Potts, B. M., 2004: Glacial refugia and reticulate evolution: the case of the Tasmanian eucalypts. *Philosophical Transactions of the Royal Society of London B: Biological Sciences*, 359: 275–284.

McVean, D. N., 1958: Snow cover and vegetation in the Scottish Highlands. *Weather*, 13: 197–200.

Mineral Resources Tasmania, 2016: *Geological polygons 1:250000*, LISTmap, http://maps.thelist.tas.gov.au/listmap/app/list/map, accessed 1 April 2016.

Minitab 17 Statistical Software, 2010: Minitab, Inc., State College, Pennsylvania, https://www.minitab.com/en-us/, accessed 2 February 2016.

Nunez, M., Kirkpatrick, J. B., and Nilsson, C., 1996: Rainfall estimation in south west Tasmania using satellite images and phytosociological calibration. *International Journal of Remote Sensing,* 17: 1583–1600.

Sass, O., Heel, M., Leistner, I., Stöger, F., Wetzel, K. F., and Friedmann, A., 2012: Disturbance, geomorphic processes and recovery of wildfire slopes in North Tyrol. *Earth Surface Processes and Landforms*, 37: 883–894.

Schneider, C. A., Rasband, W. S., and Eliceiri, K. W., 2012: NIH Image to ImageJ: 25 years of image analysis. *Nature Methods*, 9: 671–675.

Shakesby, R. A., and Doerr, S. H., 2006: Wildfire as a hydrological and geomorphological agent. *Earth-Science Reviews*, 74: 269–307.

Slee, A., Kiernan, K., and Shulmeister, J., 2015: Contemporary sorted patterned ground in low altitude areas of Tasmania. *Geographical Research*, 53: 175–183.

Slee, A., Shulmeister, J., Kiernan, K., and Jenkinson, A., 2016: Stone-banked lobes as a product of mild freeze-thaw action: an example from western Tasmania, Australia. *Geografiska Annaler: Series A, Physical Geography*, 98: 97–109.

Sturm, M., Racine, C., and Tape, K., 2001: Climate change: increasing shrub abundance in the Arctic. *Nature*, 411: 546–547.

Sturm, M., Schimel, J., Michaelson, G., Welker, J. M., Oberbauer, S. F., Liston, G. E., Fahnestock, J., and Romanovsky, V. E., 2005: Winter biological processes could help convert arctic tundra to shrubland. *Bioscience*, 55: 17–26.

Styger, J., and Balmer, J., 2009: *Alpine Treeline Ecotone Monitoring Program within the Tasmanian Wilderness World Heritage Area*. Hobart: Department of Primary Industries, Parks, Water and Environment, *Nature Conservation Report 2009/4*.

Tape, K. E. N., Sturm, M., and Racine, C., 2006: The evidence for shrub expansion in northern Alaska and the Pan-Arctic. *Global Change Biology*, 12: 686–702.

Visoiu, M., 2014: *Establishment Report for Tasmanian Wilderness World Heritage Area Climate Change Monitoring Program: Monitoring of the Expression of Feldmark Vegetation on The Boomerang, Southern Tasmania*. Hobart: Department of Primary Industries, Parks, Water and Environment, *Nature Conservation Report 14/3*.

Washburn, A. L., 1979: *Geocryology: a Survey of Periglacial Processes and Environments*. London: Edward Arnold, 406 pp.

MS submitted 2 January 2017
MS accepted 9 June 2017